Lecture Notes in Mechanical Engineering

José Machado
Filomena Soares
Justyna Trojanowska
Sahin Yildirim *Editors*

Innovations in Mechatronics Engineering

Springer

Lecture Notes in Mechanical Engineering

Lecture Notes in Mechanical Engineering (LNME) publishes the latest developments in Mechanical Engineering—quickly, informally and with high quality. Original research reported in proceedings and post-proceedings represents the core of LNME. Volumes published in LNME embrace all aspects, subfields and new challenges of mechanical engineering. Topics in the series include:

- Engineering Design
- Machinery and Machine Elements
- Mechanical Structures and Stress Analysis
- Automotive Engineering
- Engine Technology
- Aerospace Technology and Astronautics
- Nanotechnology and Microengineering
- Control, Robotics, Mechatronics
- MEMS
- Theoretical and Applied Mechanics
- Dynamical Systems, Control
- Fluid Mechanics
- Engineering Thermodynamics, Heat and Mass Transfer
- Manufacturing
- Precision Engineering, Instrumentation, Measurement
- Materials Engineering
- Tribology and Surface Technology

To submit a proposal or request further information, please contact the Springer Editor of your location:

China: Ms. Ella Zhang at ella.zhang@springer.com
India: Priya Vyas at priya.vyas@springer.com
Rest of Asia, Australia, New Zealand: Swati Meherishi at swati.meherishi@springer.com
All other countries: Dr. Leontina Di Cecco at Leontina.dicecco@springer.com

To submit a proposal for a monograph, please check our Springer Tracts in Mechanical Engineering at http://www.springer.com/series/11693 or contact Leontina.dicecco@springer.com

Indexed by SCOPUS. All books published in the series are submitted for consideration in Web of Science.

More information about this series at http://www.springer.com/series/11236

José Machado · Filomena Soares ·
Justyna Trojanowska · Sahin Yildirim
Editors

Innovations in Mechatronics Engineering

Springer

Editors
José Machado
Department of Mechanical Engineering
University of Minho
Guimarães, Portugal

Filomena Soares
Department of Industrial Electronics
University of Minho
Guimarães, Portugal

Justyna Trojanowska
Poznan University of Technology
Poznan, Poland

Sahin Yildirim
Department of Mechatronics Engineering,
Faculty of Engineering
Erciyes University
Kayseri, Turkey

ISSN 2195-4356 ISSN 2195-4364 (electronic)
Lecture Notes in Mechanical Engineering
ISBN 978-3-030-79167-4 ISBN 978-3-030-79168-1 (eBook)
https://doi.org/10.1007/978-3-030-79168-1

This Springer imprint is published by the registered company Springer Nature Switzerland AG
The registered company address is: Gewerbestrasse 11, 6330 Cham, Switzerland

Preface

This volume of Lecture Notes in Mechanical Engineering gathers selected papers presented at the first International Scientific Conference ICIE'2021, held in Guimarães, Portugal, on June 28–30, 2021. The conference was organized by School of Engineering of University of Minho, throughout MEtRICs and ALGORITMI Research Centres.

The aim of the conference was to present the latest engineering achievements and innovations and to provide a chance for exchanging views and opinions concerning the creation of added value for the industry and for the society. The main conference topics include (but are not limited to):

- Innovation
- Industrial Engineering
- Mechanical Engineering
- Mechatronics Engineering
- Systems and Applications
- Societal Challenges
- Industrial Property

The organizers received 213 contributions from 24 countries around the world. After a thorough peer review process, the committee accepted 126 papers written by 412 authors from 18 countries for the conference proceedings (acceptance rate of 59%), which were organized in three volumes of Springer Lecture Notes in Mechanical Engineering.

This volume, with the title "Innovations in Mechatronics Engineering," specifically reports on innovative control and automation concepts for applications in a wide range of fields, including industrial production, medicine and rehabilitation, education and transport, with a special focus on cutting-edge control algorithms for mobile robots and robot manipulators, innovative industrial monitoring strategies for industrial process, improved production systems for smart manufacturing, and discusses important issues related to user experience, training and education, as well as national developments in the field of mechatronics. Last but not least, it provides a timely overview and extensive information on trends and technologies behind the

future developments of mechatronics systems in the era of Industry 4.0. This book consists of 41 chapters, prepared by 147 authors from 10 countries.

Extended versions of selected best papers from the conference will be published in the following journals: Sensors, Applied Sciences, Machines, Management and Production Engineering Review, International Journal of Mechatronics and Applied Mechanics, SN Applied Sciences, Dirección y Organización, Smart Science, Business Systems Research, and International Journal of E-Services and Mobile Applications.

A special thank to the members of the International Scientific Committee for their hard work during the review process.

We acknowledge all that contributed to the staging of ICIE'2021: authors, committees, and sponsors. Their involvement and hard work were crucial to the success of ICIE'2021.

June 2021

José Machado
Filomena Soares
Justyna Trojanowska
Şahin Yildirim

Contents

Screwing Process Monitoring Using MSPC in Large Scale Smart Manufacturing

Humberto Nuno Teixeira[1](✉), Isabel Lopes[1], Ana Cristina Braga[1], Pedro Delgado[2], and Cristina Martins[2]

[1] ALGORITMI Research Centre, University of Minho, Guimarães, Portugal
b6440@algoritmi.uminho.pt
[2] Bosch Car Multimedia Portugal SA, Braga, Portugal

Abstract. The ability to obtain useful information to support decision-making from big data sets delivered by sensors can significantly contribute to enhance smart manufacturing initiatives. This paper presents the results of a study performed in an automotive electronics assembly line. An approach that uses Multivariate Statistical Process Control based on Principal Component Analysis (MSPC-PCA) was applied to early detect undesirable changes in the screwing processes performance by extracting relevant information from the torque-angle curve data. Since the data of different torque-angle curves are not aligned, the proposed approach includes the linear interpolation of the original data to enable Principal Component Analysis (PCA). PCA proved to be an appropriate technique to obtain significant information from the process variables, which consist of the successive value of the torque at constant angular intervals. Score plots and multivariate control charts were used to detect defective tightening and identify behaviors that represent inefficient tightening. This is a new approach that can be applied to effectively monitor screwing processes in the assembly of different products either periodically or in real-time.

Keywords: Multivariate Statistical Process Control (MSPC) · Principal Component Analysis (PCA) · Screwing process · Smart manufacturing

1 Introduction

Modern manufacturing systems need to provide high quality products developed in efficient, fast and cost reduced processes [1]. The increased diversity of products also implies less time to ensure that the process is capable of producing appropriate quality [2]. Problems that affect quality are often related to assembly errors [3]. There are two basic categories of assembly tasks: parts mating and parts joining. Fasteners are commonly used to join components together in industry. The screwdrivers allow tightening of threaded fasteners with a specified torque value [4]. The usage of modern equipment involves complex parameter settings of and assessment requirements [5].

Assembly process control is a complex problem whose solution must consider all the particularities and connection requirements of a given mating [6]. Therefore, a high

J. Machado et al. (Eds.): icieng 2021, LNME, pp. 1–13, 2022.
https://doi.org/10.1007/978-3-030-79168-1_1

level of process automation demands a high level of automated monitoring and control [2]. Errors detection should occur at an early stage of the process to avoid any damage and to ensure that the assembly is completed according to the requirements and specifications [7]. Thus, to prevent technical risks, it becomes important to develop methods for providing process related information to the operator [8].

Most automatic screw fastening processes are monitored using torque sensors and a target torque for a consistent assembly is usually established. However, monitoring torque alone does not ensure the required clamping force. The torque applied to provide the desired clamping force in bolted joints can differ significantly for the same bolt type due to the combined effect of several factors, such as thread and under head friction, thread deformations and variations in bolt diameter. Therefore, problems during the tightening operation must be detected to avoid wrong conclusions about the screwing process quality. To obtain more complete information about the tightening operation performance, both torque and rotation angle should be monitored [9]. The torque-angle curves provide relevant information to properly qualify the capability of tightening tools [10].

Smart manufacturing aims to support accurate and timely decision-making from real-time data delivered by sensors [11]. The quick detection of changes, particularly increases in process variability, is essential for quality control [12]. Statistical Process Control (SPC) is frequently employed to monitor and detect relevant changes in manufacturing processes [13]. When Principal Component Analysis (PCA) technique is implemented to monitor industrial processes, Hotelling's T^2 and Squared Prediction Error (SPE) statistics are used for the detection of process disturbances which can originate failures. However, although control charts allow to detect deviations from normal operating region, they do not indicate reasons for the deviations [14]. Once the fault is exposed, the contribution of each original variable for T^2 or SPE statistics can be determined based on contribution plots. The contributions plot shows the most affected variables, so that the causes can be identified and actions to bring the process to the statistical control region can be implemented [15].

The monitoring and control of screwing process parameters has been addressed by several studies [7–9, 16]. Many of the proposed methods were designed to control the screwing process of specific parts and their generalization ability has not been proven. It was also noticed that error detection effectiveness is often assessed based on simulated experiments. Furthermore, the multivariate nature of the screwing processes is not contemplated by the exiting monitoring approaches. In industrial context, the monitoring strategies for automated tightening processes are generally focused on torque, torque-angle, torque rate and variation of rate monitoring [17]. For this purpose, an individual analysis of each monitored variable is usually performed to verify their conformance to specifications during each tightening operation. The investigation of causes of variation is not an integral part of these strategies. Therefore, a more extended application in real scenarios is still needed in most cases. For this reason, methods that provide a broader understanding of the screwing processes to the operator should be developed to support the definition of more informed improvement initiatives and analyze their impact over a sequence of tightening operations. This is particularly relevant for processes with

short operating cycles, since when a change in the process is verified a high number of tightening operations can be affected.

In this paper, an approach is proposed to monitor screwing processes' through a visual representation of their performance over time and to assist the identification of factors responsible for inefficient tightening based on torque-angle curves data. This approach was tested and refined based on its application to the screwing process of an assembly line of Bosch Car Multimedia Portugal. PCA was performed using the torque-angle curves data collected by the screwing machine controller. To enable PCA, the data of different torque-angle curves were aligned by performing linear interpolations. Then, the process was monitored in different periods using multivariate control charts. The structure of the paper is organized as follows. Section 2 presents the approach steps through its application on the assembly line screwing process and the respective results. In Sect. 3, the main results of the study are discussed. Section 4 summarizes the conclusions derived from the study and presents recommendations for future research.

2 Screwing Process Monitoring and Analysis

2.1 Sample Definition

The screwing process analysis was performed using a data set composed of 12327 observations (Table 1). All observations belong to the same product type and were executed in a unique workplace. The product is an automotive electronics system which is assembled by placing seven screws according to a predetermined sequence. The overall data set includes data concerning defective ("bad") and non-defective ("good") tightening operations. The first sample includes only 7 non-sequential cases classified as "bad". These data were included in the analysis to better test the accuracy of the PCA model by considering a higher diversity of unsuccessful cases. Samples 2 to 5 are composed of sequential cases and include all operations performed in a working day.

Table 1. Description of the screwing process data samples.

Sample		1	2	3	4	5
Date		22/09/2017	29/09/2017	02/10/2017	11/10/2017	12/10/2017
Result	Good	–	2273	3189	2959	3880
	Bad	7	5	7	2	5
Number of cases		7	2278	3196	2961	3885

2.2 Data Interpolation

A preliminary analysis of original data collected from a screwdriver at regular time intervals revealed significant fluctuations in the amplitude of the rotation angle intervals (Table 2), since the angular displacement of the screw is not constant. Therefore, linear

interpolation was the method selected to align the data and generate a torque value to each rotation angle of the predefined scale. To provide a quick result, an algorithm in R code that performs linear interpolations was developed. The obtained information allows to represent the different torque-angle curves in the same scale.

Table 2. Extract from a screwing process data set.

Angle	4	6	11	15	17	21	22	28	30	35	38	39	44
Torque	10,9	11	11,1	11,2	11,5	11,6	11,7	12	12,1	12,2	12,3	12,4	12,4
Angle	51	55	58	62	72	73	83	89	93	96	99	103	106
Torque	12,3	12,4	12,6	12,8	12,9	12,8	13	13,3	13,4	13,5	13,6	13,8	13,9
Angle	1	3	4	9	14	16	20	24	28	34	37	42	45
Torque	10,3	10,4	10,4	10,4	10,6	10,4	10	9,4	9,2	9	9,1	9	9,3

In this study, the linear interpolation was performed to determine values of torque in a range between 0 and 2300° at intervals of 10°. Since the considered variables consist of the successive value of the torque at constant angular intervals (Fig. 1), a data set composed of 231 primary variables was obtained.

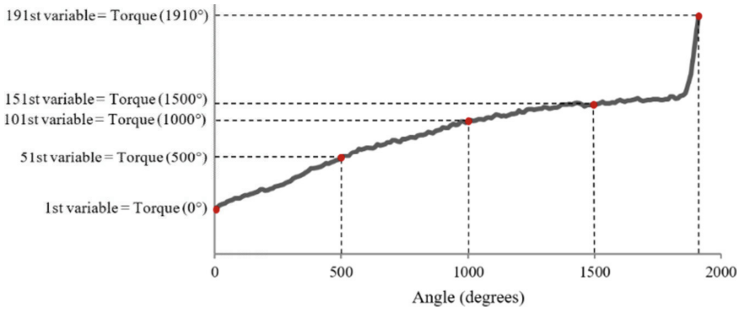

Fig. 1. Generic representation of a set of variables from a tightening operation.

2.3 Data Segmentation

The PCA model was formed by the values of 504 torque-angle curves (Fig. 2a). Only cases classified as "good" were included in the Normal Operating Conditions (NOC) data set and each screw, considering its position in the product, is represented by the same number of observations. Firstly, a set of 252 observations from a sequence of 36 consecutive products obtained in sample 3 was selected. Then, to endow the NOC data with a higher variety of behaviors, another group of 252 cases selected from samples 2 to 5 was added. Figure 2b shows three distinctive zones of a typical torque-angle curve, classified by Shoberg [17] as Rundown (R), Snugging (S) and Elastic Clamping (EC).

The torque-angle curves were represented with the Unscrambler® and the data analysis was performed using ProSensus MultiVariate software.

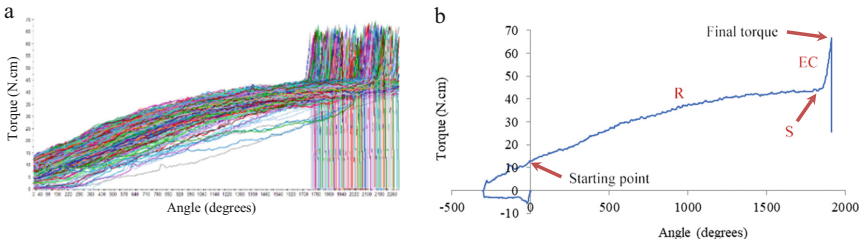

Fig. 2. NOC torque-angle curves (a) and typical torque-angle curve (b).

2.4 Principal Components Identification and Interpretation

The number of principal components extracted by the PCA model was defined based on the cumulative explained variation by the ordered components (Table 3). Since the fourth principal component has little relevance, only the first three were considered.

Table 3. Variation explained by the first four principal components.

Principal component	Variation explained	Cumulative variation explained
First	62.24%	62.24%
Second	20.40%	82.64%
Third	3.70%	86.34%
Fourth	2.06%	88.40%

The interpretation of the principal components was performed by statistics and process experts, based on the variables loadings' (Fig. 3) and considering technical knowledge about the process. In order to obtain a broader perspective of the tightening operation, the loadings of six secondary variables were also analyzed. These variables are maximum torque, absolute angle, total time, end torque, end angle and screwing energy.

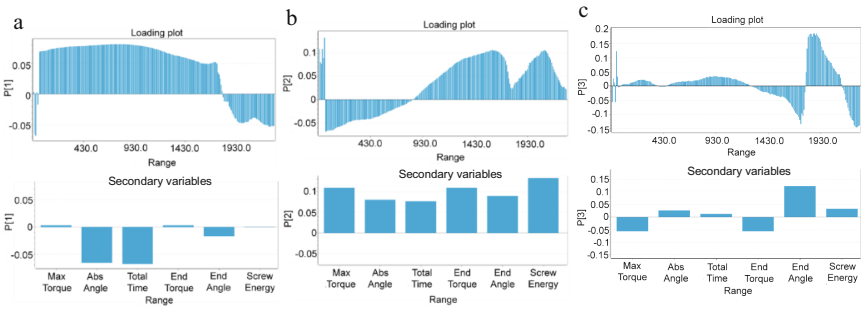

Fig. 3. Loading plots of the first (a), second (b) and third (c) principal components.

The loading plot of the first principal component (Fig. 3a) shows high loadings over the rundown zone and a significant decrease after 1740°, that represents the instant in which the snugging zone is reached. The higher loadings correspond to rotation angles wherein friction was higher. As at the elastic clamping zone, tightening is mainly affected by the elastic deformation of the screw, the corresponding variables' loadings tend to be substantially lower. After 1790°, the loadings become negative and start to assume a decreasing trend, as more tightening operations are completed. The negative loadings exhibited in this period are due to the decision of extending the tightening curves up to 0 after the final torque is achieved. The secondary variables' loadings are represented on the left side of the plot and shown with more detail below in Fig. 3a. Absolute angle, total time and end angle have negative loadings. All the other variables assume a positive correlation with the first component, since higher friction losses entail greater energy expenditure and higher torques to complete the tightening operation. However, the required clamping force is reached within a shorter period. Thus, the first principal component refers to the torque variation during the rundown zone. It allows to distinguish screws that exhibit high torques at the rundown zone, which is a behavior that can be caused by differences between screws or tighter threads.

In the second principal component loading plot (Fig. 3b), negative loadings until the angle 830 can be identified. The lowest loadings are exhibited at the beginning of the rundown zone. Afterwards, a growing trend is manifested. However, a decrease is verified in the approximation to the snugging zone and after 2090°. The secondary variables that show higher loadings are maximum torque, end torque and screw energy, since greater torques are needed to produce the required clamping force. The screwing energy loading is significantly higher in this principal component. Thus, the second principal component enables to differentiate screws that have low torques at the rundown zone, a relatively high final torque and whose tightening operation is concluded later. This behavior can be caused by more open threads due to rework, since the tightening operation must be repeated. Furthermore, this principal component also represents delays in engagement, manifested by the presence of positive loadings in the absolute angle, total time and end angle.

The third principal component loading plot exhibits several fluctuations over the entire scale of rotation angles (Fig. 3c). These shifts reflect slope variations in the torque-angle curves. Nevertheless, the loadings' value remains close to 0 along the angles that correspond to the first two-thirds of the tightening operation. Between 1260 and 1780°, the loadings become negative and reveal a decreasing trend until the snugging zone. At the snugging zone, the loadings are positive and significantly higher. Negative loadings are also obtained after 2130° when most operations were already completed. The end angle is the secondary variable which assumes the higher loading, and both end torque and maximum torque are the only variables with negative loadings. Thus, this principal component represents screws that manifest a gradual growth of the torque with some fluctuations at the rundown zone followed by an interval in which the increase of the torque ceases before the snugging zone is reached. This circumstance contributes to the delay of the tightening operation and leads to a lower end torque. In conclusion, the third principal component refers to differences between threads. The thread crests can often

exhibit irregularities or slightly different formats (e.g., rounded, sharpened, flat) that can result in sudden variations in the torque evolution.

2.5 Control Limits Definition

To identify both defective and inefficient tightening, control limits defined by the confidence intervals of 99% and 99.73% were determined and represented using ProSensus MultiVariate. In order to test the reliability of the PCA model, the defective cases were represented with the NOC observations in the Hotelling's T^2 and SPE control charts defined based on the first three principal components (Fig. 4). Both charts show all the observations classified as "bad" above the control limits. However, in the SPE control chart the distance to the limits is shorter for a set of 8 cases that reached higher torques.

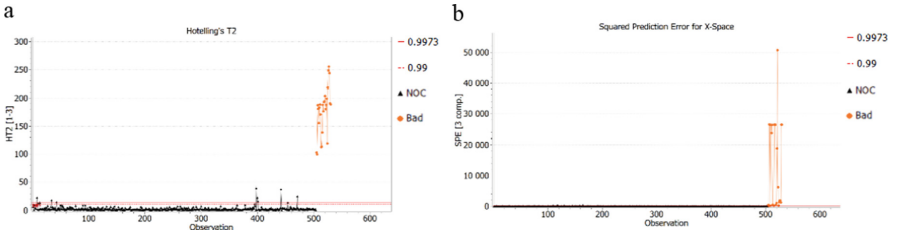

Fig. 4. Hotelling's T^2 (a) and SPE (b) control charts of the defective tightening cases.

2.6 Behavior Identification

The scatter score plot formed by the first two principal components (Fig. 5) was used to analyze the NOC observations. This analysis allowed to identify nine cases outside the limit defined by the confidence interval of 99.73%. Three correspond to significant delays at the beginning of the tightening operation (nearly 2 turns), five exhibit low torques during the entire tightening operation, and one case manifests a delay of nearly 1 turn in which the torque values are low at the rundown zone and high at the end. The first group is closer to the negative side of the first principal component axis. Whereas the second group is located at a similar distance from the negative side of both principal components' axes. These behaviors correspond to delays in engagement and well succeed reworks. The latter case is the observation that is further away from the limits. Although these behaviors resulted from special causes of variation, they cannot be completely removed. Thus, the cases that fall outside the limits were included in the NOC.

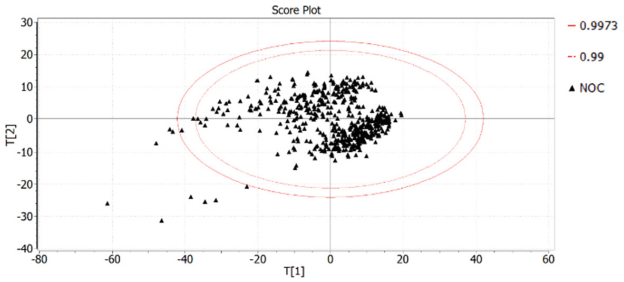

Fig. 5. Scatter score plot of the NOC observations.

2.7 Process Monitoring

The process was monitored with the data from the samples described in Table 1, except those included in the NOC. The sequential set of 11823 observations was represented in scatter score plots, time series score plots and multivariate control charts.

In the scatter score plot formed by the first two principal components several outliers were identified (Fig. 6a). The observations that deviate most from the distribution mean are the cases classified as "bad" and delays in engagement. Although this plot allows to identify unusual behaviors in each sample, it does not reveal their distribution over time. Thus, the scores were also represented in time series score plots. These plots exhibit the scores distribution over time with respect to each principal component, allowing to determine if there are any trends or fluctuations and differences between samples.

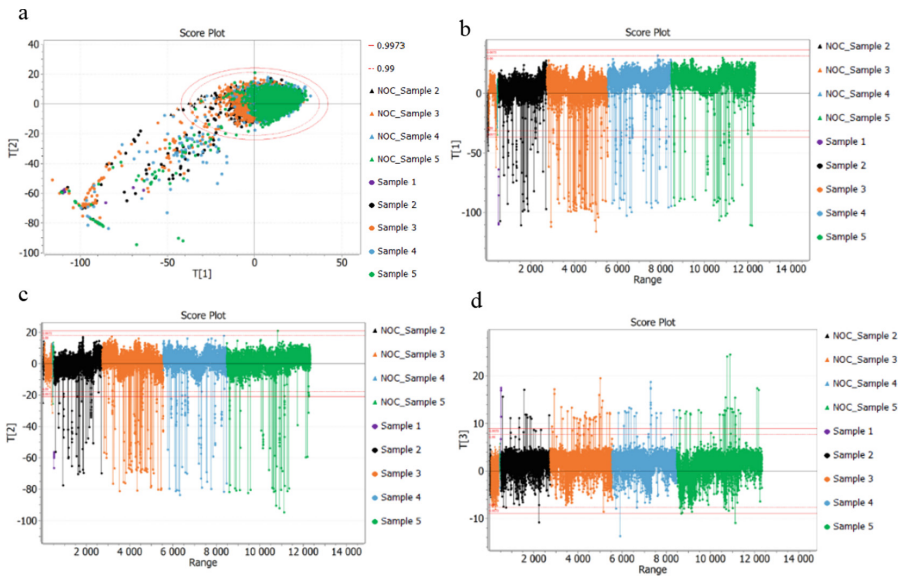

Fig. 6. Scatter score plot formed by the first two principal components (a); time series score plot of the first (b), second (c) and third (d) principal components.

In the first principal component time series score plot (Fig. 6b), several fluctuations are shown. Furthermore, the scores tend to align above the origin of the plot. However, this trend is more marked in the interval formed by the observations of samples 4 and 5. At this period, the duration of the tightening operations was shorter and higher torques at the rundown zone were attained. Since the first principal component represents the torque variation during the rundown zone, the scores of the cases with higher torques are located above the origin. In contrast, the scores that fall below the lower limit mainly correspond to defective tightening, delays and observations that exhibit low torques during the rundown zone. The scores distribution is more centered around the origin and shows lower dispersion in the second principal component time series score plot (Fig. 6c), which has lower accuracy in detecting delays. Thus, only observations that represent delays of approximately 3 turns or more comparing to the mean are outside the limits. Nevertheless, this plot is more effective in detecting observations with low torques during the entire tightening operation and shows all the defective cases below the lower limit. The existence of low torques during the rundown zone can be caused by product rework, since in most cases this behavior is verified in the torque-angle curves of the seven screws applied to the same product. The period formed by the observations of samples 4 and 5 includes a considerable number of cases with low torques at the rundown zone. This characteristic also occurs in a significant number of cases of sample 2 and is less frequent in sample 3. The third principal component time series score plot (Fig. 6d) manifests high dispersion in the scores' distribution in all the analyzed samples. However, at short periods the process becomes slightly more stable. The greater dispersion reflects a higher diversity of slope variations in the torque-angle curves. The observations identified above the upper limit comprise defective cases and the most extreme delays, whereas below the lower limit only a group of four observations that reveal very atypical variations in the torque-angle curve was detected.

The data sample in which greater instability is observed is sample 3. In the interval between observations 3435 and 3729, most of the scores lie above the origin in the plot of Fig. 6b. At the same time, a steep decrease of the scores related to the second principal component is verified and a higher number of observations below the origin is shown in the plot of Fig. 6d. Based on the analysis of the torque-angle curves that correspond to the observations of this interval (Fig. 7a) it was found that high torques are exhibited during the entire tightening operation and no delays occurred. A significant number of delays was verified thereafter in the period between observations 3730 and 4025 (Fig. 7b). This fact is reflected by the number of observations outside the limit defined by the confidence interval of 99.73% in the three time series score plots.

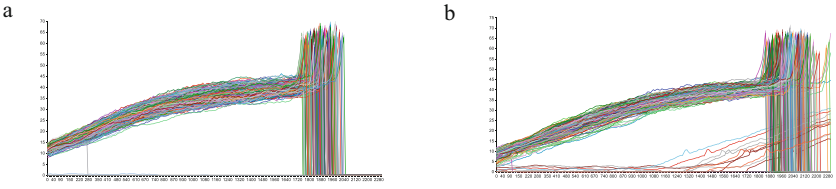

Fig. 7. Torque-angle curves: between 3435 and 3729 (a), and between 3730 and 4025 (b).

The Hotelling's T^2 control chart (Fig. 8a) shows several observations above the limits. The highest points correspond to the screwing cases classified as "bad". However, some observations which relate to delays and low torques at the rundown zone are also above the limits. In the SPE control chart (Fig. 8b), the observations which are further away from the control limits refer to defective tightening. Whereas observations that correspond to delays, although they are above the limits, reveal much lower deviations from the principal components' subspace. In addition, a small group of observations that were concluded considerably earlier are also outside the limits of this chart.

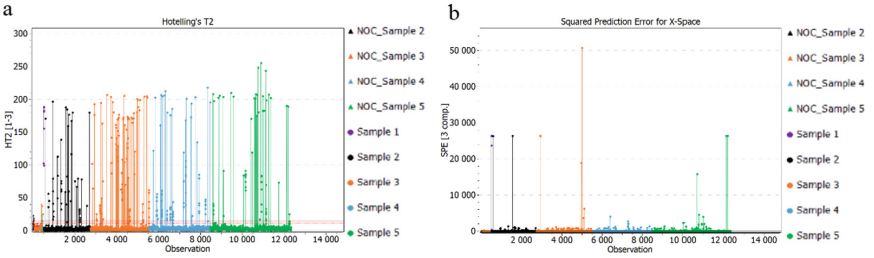

Fig. 8. Hotelling's T^2 control chart (a) and SPE control chart (b)

3 Discussion of Results

In this study, an approach for screwing processes monitoring using Multivariate Statistical Process Control based on Principal Component Analysis (MSPC-PCA) was developed and tested with data collected from a manual screwdriver of an automotive electronics assembly line. A PCA model that is deemed to represent the NOC of the process for a specific product type was defined and validated according to the proposed approach. The results show that 86.34% of the total variation can be explained only by three principal components. Since the analysis involves 231 primary variables, a univariate analysis would be extremely time consuming and would not consider correlations between variables. The interpretation of the principal components' physical meaning enabled to more accurately analyze the information provided by the monitoring tools. Moreover, it was possible to develop a detailed understanding of the process and to ascertain the causes of unusual behaviors. The structure of the principal components was partially influenced by the decision of assigning 0 to the variables that succeed the final torque to avoid missing values in the scale of rotation angles. Another option could be to maintain the value of the final torque until the end of the scale.

The time series score plots enabled to observe fluctuations in the scores' distribution, which represent sudden or gradual changes that affect the tightening behavior over time. These shifts are more visible in the first and second principal components time series score plots, since they are related to delays and increase of the number of reworks. The Hotelling's T^2 and SPE control charts show all the observations related to defective tightening above the control limits. In addition, cases that exhibit unusual behaviors, such as delays or low torques at the rundown zone, were also easily identified both in

the score plots and control charts. Some of these observations formed distinct groups of outliers in the scatter score plot of the first two principal components. Comparing both control charts, it can be verified that delays are more easily detected in Hotelling's T^2, since those cases reflect more significant deviations from the distribution mean.

MSPC-PCA can be applied using an appropriate software available in the market. If the proposed approach is used to monitor screwing processes in real-time, this functionality must also be provided by the software package. The screwdriver operator and the responsible by the screwing process should be able to monitor the process using four main tools, such as the scatter score plots formed by pairs of principal components, time series score plots concerning each principal component, Hotelling's T^2 and SPE control charts. The uncommon behaviors depicted in the scatter score plots should be promptly identified and classified considering the principal components' physical meaning and making comparisons with the NOC observations scores, namely groups that are further away from the distribution mean. Furthermore, the knowledge acquired from the PCA model definition must also be used to interpret points outside the control limits, patterns and trends both in the time series score plots and multivariate control charts. Whenever significant anomalies are detected, their causes should be investigated considering the process variables which contributed most to the identified shifts or inferred based on experience. Subsequently, appropriate corrective actions must be planned and implemented.

4 Conclusion

This paper proposes an approach that provides the ability to monitor the overall screwing process behavior over time and considers the multivariate nature of each tightening operation. The defined approach uses PCA to extract relevant information from correlated variables that consist of the successive values of the torque at constant angular intervals. Afterwards, scatter score plots, time series score plots and multivariate control charts developed based on the defined PCA model are applied to enable the process monitoring in different perspectives. The application of the proposed approach to the study data showed the capacity of these tools to detect defective tightening. Screwing cases that reveal unusual behaviors are also identified and classified. Thus, performing linear interpolations to align the screwing process data proved to be an essential and appropriate decision for the successful application of PCA.

The case study enabled to define and validate a PCA model that represents the NOC of a workplace for a specific product type. Considering the obtained results, Bosch Car Multimedia Portugal decided to monitor its screwing processes in real-time based on the defined approach. The same procedure will be adopted to define NOC models to monitor other combinations of products and workplaces. It is expected that real-time monitoring will contribute to achieve significant improvements, particularly the reduction of operating cycles due to a higher awareness to delays and the identification of components out of specifications (e.g., tighter threads, irregularities in thread crests) which can often result in defective tightening. Each NOC model must be updated whenever adjustments are made in the process. This task requires considerable time and effort from the people involved. Therefore, the ability to perform self-adaptive model updating is highly desirable in this context. The PCA model used to enable the MSPC is based on data related

to screws placed in seven different positions. In order to guarantee greater homogeneity, a PCA model for each screw joint can be defined. However, a more significant technical and human effort would be needed to coordinate the process monitoring due to the increase of the amount of data and tools involved.

Future work will address the development of an automatic classifier which performs feature recognition of the screwing process observations and their prompt association to specific behavior categories. Furthermore, it is intended to identify patterns or trends in the monitored data that can be associated with failure modes of the screwing equipment by analyzing the process evolution over time. Afterwards, this information will be used to prevent or early detect failures in the screwing equipment.

Acknowledgements. This work has been supported by FCT – Fundação para a Ciência e Tecnologia within the R&D Units Project Scope: UIDB/00319/2020.

References

1. Foehr, M., Lüder, A., Wagner, T., Jäger, T., Fay, A.: Development of a method to analyze the impact of manufacturing systems engineering on product quality. In: 2011 IEEE 16th Conference on Emerging Technologies & Factory Automation (ETFA), Toulouse, France, pp. 1–4. IEEE (2011)
2. Wolter, B., Dobmann, G., Boller, C.: NDT based process monitoring and control. Strojniški Vestn. – J. Mech. Eng. **57**, 218–226 (2011)
3. Tsarouchi, P., et al.: Robotized assembly process using dual arm robot. Procedia CIRP **23**, 47–52 (2014)
4. Longwic, R., Nieoczym, A.: Control of the process of screwing in the industrial screwdrivers. Adv. Sci. Technol. **10**, 202–206 (2016)
5. Yuliya, L., Ulrich, B.: Development of an information system with maturity degree management for automated screwing processes. In: Nunes, M.B., Isaías, P., Powell, P. (eds.) Proceedings of the IADIS International Conference Information Systems 2012, pp. 49–56. IADIS Press, Berlin (2012)
6. Chumakov, R.: Optimal control of screwing speed in assembly with thread-forming screws. Int. J. Adv. Manuf. Technol. **36**, 395–400 (2008)
7. Deters, C., Lam, H.K., Secco, E.L., Wurdemann, H.A., Seneviratne, L.D., Althoefer, K.: Accurate bolt tightening using model-free fuzzy control for wind turbine hub bearing assembly. IEEE Trans. Control Syst. Technol. **23**, 1–12 (2015)
8. Lebedynska, Y., Berger, U.: Intelligent knowledge-based system for the automated screwing process control. In: Proceedings of the 11th WSEAS International Conference on Artificial Intelligence, Knowledge Engineering and Data Bases (AIKED 2012), Cambridge, pp. 175–180 (2012)
9. Saygin, C., Mohan, D., Sarangapani, J.: Real-time detection of grip length during fastening of bolted joints: a Mahalanobis-Taguchi system (MTS) based approach. J. Intell. Manuf. **21**, 377–392 (2010)
10. Cristalli, C., et al.: Integration of process and quality control using multi-agent technology. In: 2013 IEEE International Symposium on Industrial Electronics, Taipei, Taiwan, pp. 1–6 (2013)
11. He, Q.P., Wang, J.: Statistical process monitoring as a big data analytics tool for smart manufacturing. J. Process Control. **67**, 35–43 (2018)

12. Yeh, A.B., Li, B., Wang, K.: Monitoring multivariate process variability with individual observations via penalised likelihood estimation. Int. J. Prod. Res. **50**, 6624–6638 (2012)
13. Siddiqui, Y.A., Saif, A.-W., Cheded, L., Elshafei, M., Rahim, A.: Integration of multivariate statistical process control and engineering process control: a novel framework. Int. J. Adv. Manuf. Technol. **78**(1–4), 259–268 (2014). https://doi.org/10.1007/s00170-014-6641-6
14. Lin, W., Qian, Y., Li, X.: Nonlinear dynamic principal component analysis for on-line process monitoring and diagnosis. Comput. Chem. Eng. **24**, 423–429 (2000)
15. Babamoradi, H., van den Berg, F., Rinnan, A.: Confidence limits for contribution plots in multivariate statistical process control using bootstrap estimates. Anal. Chim. Acta. **908**, 75–84 (2016)
16. Mura, M.D., Dini, G., Failli, F.: An integrated environment based on augmented reality and sensing device for manual assembly workstations. Procedia CIRP **41**, 340–345 (2016)
17. Shoberg, R.S.: Engineering Fundamentals of Threaded Fastener Design and Analysis. RS Technologies, a Division of PCB Load & Torque, Inc., Farmington Hills (2000)

Comparison of Neural Networks Aiding Material Compatibility Assessment

Izabela Rojek[1(✉)], Ewa Dostatni[2], and Piotr Kotlarz[1]

[1] Institute of Computer Science, Kazimierz Wielki University, Bydgoszcz, Poland
izarojek@ukw.edu.pl
[2] Faculty of Mechanical Engineering, Poznan University of Technology, Poznan, Poland

Abstract. A new method of selection of materials at the design step is presented in this paper. The method takes into recyclability of materials. The authors compare the effectiveness of neural networks (a multilayer perceptron, radial basis function networks, and self-organizing feature map - SOFM networks) as modelling tools aiding the selection of compatible materials in ecodesign. The best artificial neural networks were used in an expert system. The input data for the selection of materials was start point to initiate the study. The input data, specified in cooperation with designers, include both technological and environmental parameters which guarantee the desired compatibility of materials. Next, models were developed using the selected neural networks. The models were assessed and implemented into an expert system. The authors show which models best fit their purpose and why. Models aiding the compatible materials selection help boost the recycling properties of designed products. Neural networks are a very good tool to support the selection of materials in the ecodesign. This has been proven in the article.

Keywords: Compatibility · Neural networks · Classification models · Expert system · Materials selection

1 Introduction

Nowadays, fast development of environmental awareness is observed. Enterprises are increasingly focusing on environmentally friendly solutions due to legal regulations. Producers' attitudes are also shaped by marketing campaigns that promote eco-friendly products. Creating customer demand, they force manufacturers to supply eco-friendly products to the market. Some customer groups due to greater awareness are even willing to pay a higher price for an eco-friendly product. Manufacturers also sell products in ecological versions cheaper.

The study, exploring the materials selection in ecodesign, is a follow up on previous research into the application of artificial intelligence (AI) in the selection of materials in product design to provide for their recycling compatibility. The research has been described in [1–4]. Based on the decision tree induction methods and MLP artificial neural networks, the proposed tools automate the materials selection in the process of design, building upon the designer's knowledge gained through experience.

J. Machado et al. (Eds.): icieng 2021, LNME, pp. 14–24, 2022.
https://doi.org/10.1007/978-3-030-79168-1_2

A new method supporting designers at the design stage in choosing materials that are compatible ensures that the product is recyclable and environmentally friendly. The aim of the authors study was to create expert system similar to human thinking in the concept of reasoning. Functions of the created expert system allows to solve certain tasks, in the similarly like a man who is an expert in the domain. The creation of such a system was possible to the use of artificial neural network methods.

2 Review of Literature

The ecodesign concept combines many aspects of traditional and environmental design. The main goal is to develop sustainable solutions that meet human needs [5]. Product recyclability is one of the basis of ecodesign. Recycling is one of the methods of environmental protection. It consists to reduce the amount of waste and the consumption of natural resources [6]. Therefore, at the initial stages of the product life cycle, you should consider what will happen to it after its end of life.

More and more ecodesign supporting tools use intelligent solutions, such as neural networks. The article [7] presents models of life cycle assessment (LCA) based on a BPNN, which allow estimating the amount of hazardous chemicals and the consumption of electronic product for the entire product lifecycle. The solution described in [8] uses the artificial neural network (ANN) for forecasting and performance of product lifecycle assessment (LCA). Any missing data required for the LCA is estimated using the ANN. Artificial intelligence is also applied in waste sorting is the deep learning based method, implemented by Refined Technologies of Sweden [9]. It recognizes products or product models with a high degree of similarity.

Many researchers have described the application of neural networks methodologies across different scientific and practical domains. Numerous research papers discuss Kohonen networks applied for multidimensional data visualization to evaluate classification possibilities of various coal types [10], collision free path planning and control of wheeled mobile robot [11], or parametric fault clustering in analog electronic circuits with the use of a self-organizing artificial neural network [12].

Radial basis function (RBF) networks are also widely discussed in the literature as a tool supporting, among others, rotor fault detection of the converter fed induction motor [13], local dynamic integration of ensemble in prediction of time series [14], predicting the corrections of the Polish time scale UTC(PL) (Universal Coordinated Time) [15], or accurate load forecasting in a power system [16]. However, solutions implementing the RBFN, Kohonen networks or MLP in ecodesign are scarce. Hence the authors' interest in the application of neural networks.

The method aiding the selection of materials in the ecodesign, which used neural networks was shown in the article. While developing the expert system, the authors used their experience from solutions supporting ecodesign [17–19] and creative of neural networks [4, 20–22].

3 Methods

Materials selection for product components is aided with the use of MLP, RBF and SOFM networks. Neural networks are very good suited to the obtain of knowledge and

experience, in this case in the range of selection of compatible materials in the process of ecodesign.

The MLP network structure consists of many artificial neurons in a few connected layers. The artificial neural network is a very simplified model of the brain of a living organism, because the brain doesn't have a perfectly layered structure in which neurons are connected between the layers. The neural network model is very simplified. For simpler implementation, the neural network is built symmetrically. It consists in the fact that all neurons from one layer are connected to neurons of the next layer. The network learning process eliminates connection redundancy [23]. MLP networks have three basis features. The network is made up of layers in which neurons are located. These neurons in each layer may have a different number. The layers in the network connect to each other on the principle of: each neuron from one layer with each neuron of the previous layer. Data in the network flows from entry to exit in one direction. The network can be divided into input, hidden (or n hidden) and output layers.

MLP network is the most universal network commonly applied for resolving various problems, including technical ones [23]. But, RBF networks also have many advantages. Firstly, they are able to map any nonlinear function by a single hidden layer, unlike the MLP network where sometimes we need more than one hidden layer. Moreover, the RBF network typically has one hidden layer with radial neurons, each of which models the Gaussian process based response surface [23]. Radial networks are composed of neurons whose activation functions map (1). Their values change radially around center c.

$$x \to \varphi(\|x - c\|), \ x \in R^n \tag{1}$$

where $(\|\cdot\|)$ is usually typically an Euclidean norm. Functions $\varphi(\|x - c\|)$ are referred to as radial basis functions.

Secondly, in the output layer we can performed to optimize simple linear transformation by means of traditional linear modelling techniques. The techniques are quick and free from such problems as local minima, which occur in the training of MLP networks. Therefore, we can train RBF networks in a very short time period (the difference in the training speed can reach orders of magnitude).

Kohonen networks are one of the basic types of self-organizing networks. They train in a way similar to the way human beings do, without defining any patterns – the patterns are created through the training process combined with normal functioning. Owing to their self-organizing capability, they open up new possibilities, such as adaptation to input data they have little knowledge of. SOFM networks represent an entire group of networks which learn by the self-organizing competitive method. On the network's inputs signals are set up to choose the winning neuron – the one which best corresponds to the input vector. SOFM's topology correct feature maps first choose the winning neuron (by means of the Euclidean distance), and subsequently determine the training coefficient of the winner's neighboring neurons [23].

Once the network is triggered by the input vector x, neurons compete among themselves. The winning neuron is the one whose weights are most similar to the respective components of that vector. A topological neighborhood G(i, x) is assumed around the i^{th} neuron. In the standard Kohonen algorithm, the G(i, x) function is defined as follows (2):

$$G(i,x) = \begin{cases} 1 \, for \, d(i,w) \leq R \\ 0 \, for \, others \end{cases} \tag{2}$$

where d(i, w) represents the Euclidean distance between the winning vector w_i and the i^{th} neuron, and R – the neighborhood radius.

We identify three stages in Kohonen networks: construction, learning, and recognition.

4 Creation of Models Based on the Neural Networks

The selection of materials in the ecodesign is possible thanks to neural network models that were created in the following stages:

- analysis of input data for the selection of the materials (input data were developed on the basis of real data taken into account by the designers when selecting materials),
- creating training, testing and validation kits containing examples of the selection of materials to be used in creating neural networks and evaluation their effectiveness,
- creating models using neural networks (MLP, RBF, SOFM),
- model evaluation,
- selection of the most effective material selection models and their implementation in the expert system.

4.1 Data Preparation

Recycling oriented ecodesign relies primarily on the material selection and methods of connecting them. The main goal is to design a product made of the largest possible number of standardized and recyclable materials. This has a positive impact on the environment in the last stages of the product's lifecycle, such as maintenance or withdrawal from use. When selecting materials for a product, we are guided by their compliance in terms of recycling. Mainly the chemical composition of materials determines recycling. Special tables have been developed that show material compatibility due to recycling.

For a detailed analysis, selected properties of materials have been added upon consultation with designers. Parameters of material selection were chosen for AGD products. The files have been prepared based on an analysis of properties of materials, such as: MM - main material name (e.g. PVC), D - density in grams per cubic centimeter (e.g., 7.88), TS - tensile strength expressed in mega Pascal (e.g., 35.5), YPE - elongation at yield point (Re) expressed as a percentage value (e.g., 5.5), PT - processing temperature expressed in degrees centigrade (e.g., 20.8), DC - the dielectric constant (e.g., 2.0), ME - Young's modulus (elasticity) expressed in gigapascal (e.g., 4.61), WA - water absorbency

expressed as a percentage value (e.g., 22.55), RC - the recycling cost expressed in PLN per kilogram (e.g., 4.25), where a positive value represents a profit from the sale of material, and a negative one – the disposal cost, and AM - the added material name (e.g. ABS). Properties of materials give inputs of MLP network and output is C - compatibility. The data set includes 980 examples.

4.2 Material Selection by Neural Networks

In experiments authors built many models of MLP neural networks. The input and output of the network was the same for all built models (10 inputs and 1 output) (see Fig. 1). In order to develop the best model of the neural network, various parameters were changed in the experiments. Changed: the number of neurons in the hidden layer (5–25), in the BFGS algorithm the number of training periods (10–120), the error function (SOS, Entropy), the activation function in the hidden and output layer (linear, logistic, exponential, Tanh, Softmax). Seven neural networks of varying efficacy (activity quality) were presented in Table 1.

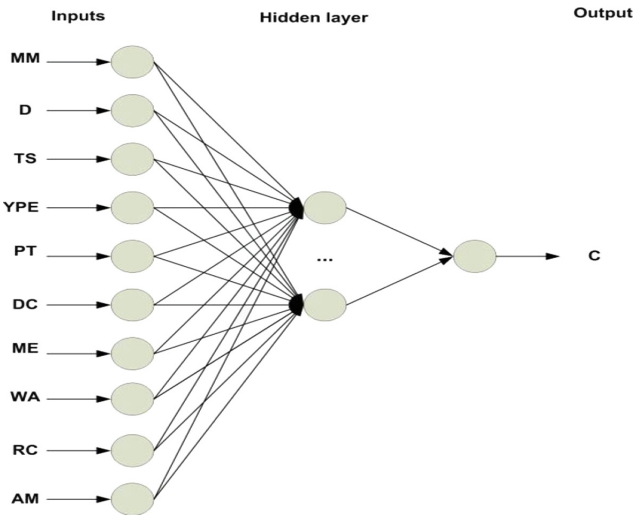

Fig. 1. MLP network structure.

MLP 10-23-1, MLP 10-16-1, and MLP 10-21-1 neural networks were the most effective neural networks (100%). MLP 10-25-1 (96.87%), MLP 10-9-1 (97.12%), MLP 10-16-1 (99.22%), and MLP 10-25-1 (96.34%) neural networks were a little less effective. MLP 10-12-1 turned out to be the least effective (76.48%). Table 2 shows the analysis of neural network errors. In the case of networks with lower efficiency, these networks classified some examples incorrectly.

The MLP 10-23-1 network had 0% errors (100%, best network). MLP 10-25-1 was slightly worse (35 errors) and MLP 10-12-1 showed the worst classification (220 errors).

Table 1. The neural networks (MLP) models for material selection.

ID	S	TQ	TEQ	VQ	TA	FE	FHA	FOA
1	10-25-1	96.06	97.96	96.60	38	Entropy	Logistic	Softmax
2	10-23-1	100.00	100.00	100.00	80	SOS	Tanh	Linear
3	10-16-1	100.00	100.00	100.00	30	Entropy	Tanh	Softmax
4	10-9-1	96.79	97.96	96.59	57	Entropy	Logistic	Softmax
5	10-16-1	95.19	96.59	95.24	35	Entropy	Logistic	Softmax
6	10-25-1	96.50	97.95	94.56	39	Entropy	Logistic	Softmax
7	10-21-1	100.00	100.00	100.00	60	SOS	Logistic	Tanh

where: ID – network of id, S – MLP network structure, TQ - quality of training, TEQ – quality of testing, VQ – quality of validation, TA - BFGS algorithm, FE - function of error, FHA – function of hidden activation, FOA – function of output activation

Table 2. Analysis of neural network errors.

Answer of network	Compatibility		
	Good	Incompatible	Limited
10-25-1-good	265	5	0
10-25-1-incompatible	10	170	15
10-25-1-limited	5	0	510
10-23-1-good	**280**	**0**	**0**
10-23-1-incompatible	**0**	**175**	**0**
10-23-1-limited	**0**	**0**	**525**
10-12-1-good	225	30	75
10-12-1-incompatible	10	115	30
10-12-1-limited	45	30	420

For RBF networks, the input parameters (10 inputs) for the construction of a neural network include material properties, including eco-friendliness, the added material for the assessment of compatibility with the main material, and one output – the decision class, which in this case is the compatibility of materials. Table 3 shows the most important data of the material selection models developed as RBF networks. The models have different numbers of neurons in the hidden layer (20–60). The activation function in the hidden layer is the Gaussian function, the activation function in the output layer is the Softmax function, and the training algorithm (RBFT).

The best RBF network (10-58-1) reached an efficiency of 94.91%. It featured 10 inputs, 58 neurons in the hidden layer, and one output. Measured with cross entropy (CE), the training error was 0.3956, the testing error – 0.2954, and the validation error – 0.3512.